Blaen, P. J., Khamis, K., Lloyd, C., Comer-Warner, S., Ciocca, F., Thomas, R. M., MacKenzie, A. R., & Krause, S. (2017). High-frequency monitoring of catchment nutrient exports reveals highly variable storm event responses and dynamic source zone activation. *Journal of Geophysical Research: Biogeosciences*, *122*(9), 2265-2281. https://doi.org/10.1002/2017JG003904

AGU PUBLICATIONS

JGR

Journal of Geophysical Research: Biogeosciences

RESEARCH ARTICLE
10.1002/2017JG003904

Key Points:
- High-frequency river monitoring using in situ sensors reveals variability in nutrient dynamics between and during storm events
- Nutrient dynamics during storm events are predicted by hydroclimatological variables and antecedent conditions
- Conceptual model of controls on nutrient-specific source zone activation presented to explain patterns of catchment nutrient export

Supporting Information:
- Supporting Information S1

Correspondence to:
P. J. Blaen,
p.j.blaen@bham.ac.uk

Citation:
Blaen, P. J., K. Khamis, C. Lloyd, S. Comer-Warner, F. Ciocca, R. M. Thomas, A. R. MacKenzie, and S. Krause (2017), High-frequency monitoring of catchment nutrient exports reveals highly variable storm event responses and dynamic source zone activation, *J. Geophys. Res. Biogeosci.*, *122*, 2265–2281, doi:10.1002/2017JG003904.

Received 18 APR 2017
Accepted 18 AUG 2017
Accepted article online 25 AUG 2017
Published online 7 SEP 2017
Corrected 5 OCT 2017

The copyright line for this article was changed on 5 OCT 2017 after original online publication.

High-frequency monitoring of catchment nutrient exports reveals highly variable storm event responses and dynamic source zone activation

Phillip J. Blaen[1,2], Kieran Khamis[1], Charlotte Lloyd[3], Sophie Comer-Warner[1], Francesco Ciocca[1,4], Rick M. Thomas[1,2], A. Rob MacKenzie[1,2], and Stefan Krause[1,2]

[1]Geography, Earth and Environmental Science, University of Birmingham, Edgbaston, UK, [2]Birmingham Institute of Forest Research, University of Birmingham, Edgbaston, UK, [3]Organic Geochemistry Unit, Bristol Biogeochemistry Research Centre, School of Chemistry, University of Bristol, Bristol, UK, [4]Silixa Ltd., Elstree, UK

Abstract Storm events can drive highly variable behavior in catchment nutrient and water fluxes, yet short-term event dynamics are frequently missed by low-resolution sampling regimes. In addition, nutrient source zone contributions can vary significantly within and between storm events. Our inability to identify and characterize time-dynamic source zone contributions severely hampers the adequate design of land use management practices in order to control nutrient exports from agricultural landscapes. Here we utilize an 8 month high-frequency (hourly) time series of streamflow, nitrate (NO_3-N), dissolved organic carbon (DOC), and hydroclimatic variables for a headwater agricultural catchment. We identified 29 distinct storm events across the monitoring period. These events represented 31% of the time series and contributed disproportionately to nutrient loads (42% of NO_3-N and 43% of DOC) relative to their duration. Regression analysis identified a small subset of hydroclimatological variables (notably precipitation intensity and antecedent conditions) as key drivers of nutrient dynamics during storm events. Hysteresis analysis of nutrient concentration-discharge relationships highlighted the dynamic activation of discrete NO_3-N and DOC source zones, which varied on an event-specific basis. Our results highlight the benefits of high-frequency in situ monitoring for characterizing short-term nutrient fluxes and unraveling connections between hydroclimatological variability and river nutrient export and source zone activation under extreme flow conditions. These new process-based insights, which we summarize in a conceptual model, are fundamental to underpinning targeted management measures to reduce nutrient loading of surface waters.

1. Introduction

Riverine nutrient loading (N, P, and C) is increasing in many catchments worldwide due to changes in land management, farming practices, and increasing urbanization [*Gruber and Galloway*, 2008; *Burt et al*., 2010; *Thomas et al*., 2016]. The resulting eutrophication of waterbodies often leads to changes in pH, turbidity, and dissolved oxygen availability, and thus, can be detrimental to aquatic ecosystem structure and functioning [*Smith and Schindler*, 2009; *Friberg et al*., 2010]. In addition to ecological impacts, high riverine nutrient concentrations can cause significant socio-economic implications by impairing freshwater ecosystem services including drinking water supply, recreational opportunities, and aesthetic qualities such as taste or odor [*Millennium Ecosystem Assessment*, 2005; *Bennett et al*., 2009]. Moreover, drinking water supplies with high concentrations of nitrate and disinfectant by-products (associated with the removal of aromatic dissolved organic matter) have been linked to adverse public health impacts including cancer, diabetes, and mutagenic diseases [*Ward et al*., 2005; *Carpenter et al*., 2013; *Ritson et al*., 2014]. Given the global relevance of increasing river nutrient concentrations, there is a critical need to develop a thorough mechanistic understanding of the variability and controls on nutrient mobilization and export from river catchments. In particular, identification of the dominant landscape source zones that contribute to nutrient export is often challenging [*Bishop et al*., 1994; *Pacific et al*., 2010; *Grabs et al*., 2012], despite the importance of this for their effective management.

Riverine nutrient concentrations can exhibit highly dynamic and nonlinear behavior [*Krause et al*., 2015] that has been observed over a wide range of temporal scales [*Bowes et al*., 2009; *Wade et al*., 2012; *Halliday et al*., 2015; *Bieroza et al*., 2014]. Traditional approaches to nutrient monitoring, constrained by laboratory and

personnel costs, were restricted to relatively coarse temporal sampling resolutions (i.e., days to weeks), although a growing body of evidence now suggests that short-term (event-based) variability in nutrient concentrations is not captured by infrequent sampling regimes [*Bowes et al*., 2009]. Recent developments in optical sensor technology are now enabling in situ, continuous measurements of riverine nutrient dynamics at subhourly temporal resolutions [*Blaen et al*., 2016]. Such high-resolution data have the potential to adequately monitor the real dynamic behavior of catchment nutrient exports and, thus, improve estimates of nutrient loads and facilitate detailed new insights into the patterns, drivers, and organizational principles of catchment nutrient fluxes.

Studies of riverine nutrient dynamics have shown that catchment exports are linked strongly to changes in hydrological and climatological conditions. For example, precipitation inputs can play an important role in determining nutrient loads by flushing solutes from near-stream sources [*Huang and Chen*, 2009]. Moreover, antecedent soil moisture, temperature, and groundwater conditions can alter the potential for transformation (e.g., mineralization) and accumulation of nutrients in shallow subsurface flow paths [*Agehara and Warncke*, 2005]. In particular, extreme flow conditions caused by episodic storm events and seasonal snowmelt have been shown to exert major influences on nutrient export patterns and dynamics [*Pellerin et al*., 2012; *Saraceno et al*., 2009; *Basu et al*., 2010; *Khamis et al*., 2017]. During these events, changes in surface and subsurface flow paths can modify riparian connectivity to the river catchment and lead to the activation of distant solute and particulate source zones that would not usually contribute to catchment nutrient export under base flow conditions. Storm events therefore may trigger hydrological and hydrochemical "hot moments" that contribute specifically to nutrient dispersal and exports from catchments. Therefore, understanding how nutrients are mobilized and transported from different source zones during these periods is critical to produce accurate estimates of the timing and magnitude of catchment nutrient fluxes in support of adequate and efficient integrated catchment water quality management [*Wilson et al*., 2013; *Carey et al*., 2014]. Such information is also needed to generate predictions of how river nutrient loads and catchment exports are likely to change under future climate regimes. This latter point is particularly important given that most climate change scenarios suggest an increase in the magnitude and frequency of episodic precipitation events and soil drying through drought across many areas of the world [*Kendon et al*., 2014; *Mann et al*., 2017], particularly where local temperatures are $<$25°C [*Wang et al*., 2017], which in turn are likely to drive changes in other hydrological variables that influence nutrient flux and in-channel processing through river catchments [*Garner et al*., 2015].

Previous studies characterizing variability in responses of catchment nutrient exports to storm events have focused mainly on single parameters, such as nitrate [*Chen et al*., 2012; *Carey et al*., 2014], fluorescent dissolved organic matter [*Saraceno et al*., 2009], or phosphate [*Bowes et al*., 2005], although in recent years a growing number have considered varying responses between nutrient types [*Drewry et al*., 2009; *Pellerin et al*., 2012; *Outram et al*., 2014]. Moreover, very few studies have investigated how changes in hydroclimatology, both during and preceding storm events, control river nutrient export and source zone activation under extreme flow conditions, despite a clear requirement for this information for the effective management of catchment water resources both now and under future climate regimes. Headwater rural catchments dominated by agricultural land use are often important sources of riverine nutrient pollution, particularly nitrogen [*Mellander et al*., 2012], and therefore, understanding controls on nutrient fluxes from these areas is an important component of developing strategies to prevent and mitigate excess nutrient loading of downstream ecosystems.

To address this research gap and provide detailed mechanistic system-level understanding of variable storm event controls on nutrient source zone activation and catchment export, we analyzed high-resolution records of streamflow, nitrate (NO_3-N), dissolved organic carbon (DOC), and a suite of hydroclimatological variables from a headwater agricultural stream. We hypothesized that (i) storm events would contribute disproportionately to nutrient export, with loads scaling with event duration; (ii) hydroclimatological variables would be significant predictors of interevent variability in nutrient export, and (iii) differences in nutrient distribution within the catchment (i.e., spatially explicit zones of NO_3-N in arable fields versus more uniform distribution of DOC) would be reflected in nutrient export patterns at the catchment outlet (stronger hysteretic behavior for NO_3-N than DOC), providing an inverse approach to learn about source zone activation from observed nutrient export at the catchment outlet.

2. Methods

2.1. Site Description

Catchment nutrient exports were analyzed for the Wood Brook at the Birmingham Institute of Forest Research (www.birmingham.ac.uk/bifor) field site in the UK between March and November 2016 (Figure 1). This second-order stream drains a 3.1 km^2 catchment ranging elevation from 90 to 150 m above mean sea level and is situated in a nitrate vulnerable zone (a conservation designation for land draining into nitrate-polluted waters; Directive 91/676/EEC). Land use was dominated by arable farming of potatoes and winter wheat and a mixture of young and mature deciduous woodland, primarily English oak (*Quercus robur*), hazel (*Corylus avellana*), hawthorn (*Crataegus* spp.), and sycamore (*Acer pseudoplatanus*). Young woodland areas were planted with saplings in 2014, prior to which the land was used for arable farming for more than 20 years. Tile drains are present in some arable and young woodland areas of the catchment. In spring 2016, arable farmland areas were dosed repeatedly with soil fertilizer (ammomium nitrate and ammonium sulfate) with application rates of 45–80 kg N/ha, which are typical for these crop types in the UK [e.g., *Outram et al*., 2014]. Mean annual temperature at the site is 9°C, and mean annual precipitation is 690 mm [*Norby et al*., 2016]. Catchment geology is composed of red Permo-Triassic sandstone overlain by superficial deposits of glacial till up to 10 m thick, with organic-rich, sandy clay topsoils between 0.15 and 0.6 m thick.

2.2. Stream Water Sampling

A stream water quality monitoring station was deployed at the catchment outflow to provide continuous in situ measurements of water and nutrient fluxes (Figure 1). The station was equipped with a pressure transducer (Adcon, Austria) for stage measurements, an OPUS UV spectral sensor (TriOS GmbH, Germany) for optical measurements of NO_3-N and DOC concentrations, and a Manta 2 multiprobe (Eureka, TX, USA). The Manta 2 was equipped with sensors for ancillary measurements of water temperature, electrical conductivity, and turbidity. A stage-discharge relationship (R^2 = 0.89; Figure S1 in the supporting information) was derived from salt dilution gauging measurements [*Hudson and Fraser*, 2005] and was consistent throughout the study period.

Channel geometry and restrictions in water depth of this second-order stream meant that most sensors (except the pressure transducer) were not submerged in the stream but housed in an insulated kiosk 1 m from the stream bank. An ISCO (Lincoln, NE, USA) 3710 peristaltic pump was used to pass 1 L of water every hour from an intake point in the thalweg of the stream through two flow cells containing the OPUS UV sensor and Manta 2, respectively. The intake was protected with a coarse (1 mm) nylon mesh to prevent damage to the pump tubing from large particulates. Instruments were programmed to acquire sample readings 3 min after the completion of each pumping cycle. Data were uploaded every 3 h via a telemetry system to an internet server for storage and quality control.

All sensors were cleaned every 2 to 4 weeks using acetone on optical windows and mild detergent on other components. Tubing was flushed with 10% HCl on each cleaning occasion to inhibit the development of biofilms. In addition, the Manta 2 had an automatic wiper that cleaned all sensors every 10 min throughout the monitoring period. Grab samples were collected to validate and adjust NO_3-N and DOC readings by in situ sensors, with efforts focusing on storm events when concentration range was greatest. Therefore, an ISCO 3700 autosampler was used to collect hourly samples during storm events (n = 83), while additional manual grab samples were collected throughout the monitoring period (n = 13). All samples were filtered through 0.45 μm nylon filters (Thames Restek, UK) into sterile HDPE bottles, kept cool, and frozen within 6 h for later analysis using a Skalar (Breda, Netherlands) SAN++ continuous flow analyzer for NO_3-N and a Shimadzu (Kyoto, Japan) TOC-L analyzer for DOC.

2.3. Hydroclimatological Sampling

Hydroclimatological variables were measured continuously throughout the study period to provide insights into the environmental processes that drive variability in water and nutrient fluxes at the catchment outflow. The aim was not to characterize the full range of spatial variability within the catchment, but rather the relative temporal changes in local hydroclimatological conditions that occurred between storm events. Therefore, precipitation was measured every 15 min using an ARG100 tipping bucket rain gauge (EML, UK) positioned in the center of the catchment (elevation 110 m above sea level (asl)) and away from trees or other structures which could influence collection at a distance >1.5 times the height of the nearest object.

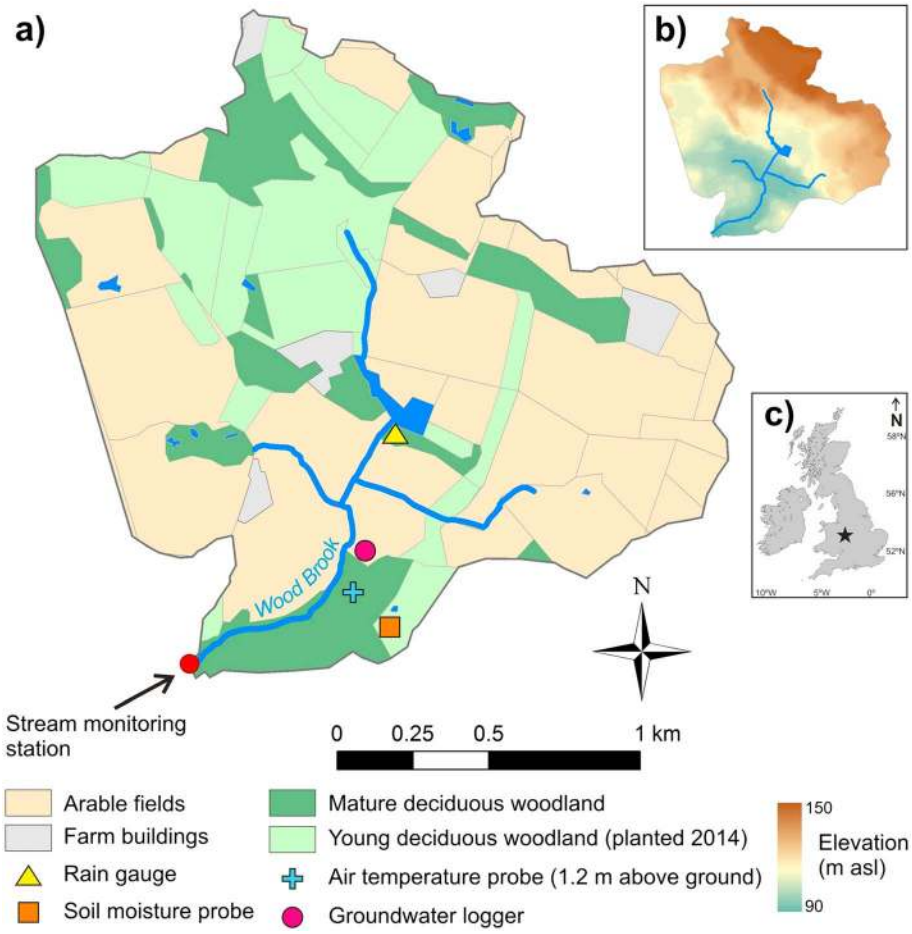

Figure 1. Map of catchment showing (a) location of stream monitoring station and dominant land cover distribution, (b) land surface elevation, and (c) location within the UK.

Volumetric soil moisture content at 10 cm depth was measured at 15 min intervals using a 5TM probe (Decagon Devices, WA, USA) positioned in a young woodland clearing in the south of the catchment (elevation 100 m asl). Air temperature was measured every 15 min using a Vaisala HMP155 probe positioned on a meteorological monitoring tower at 1.2 m above the ground in the south of the catchment. Groundwater levels were recorded hourly using a Mini-Diver (Van Essen Instruments B.V., Netherlands) located in a 10 m deep borehole in the south of the catchment. Comparison of precipitation, soil moisture, air temperature, and groundwater measurements showed good agreement (typically $r > 0.9$, $p < 0.01$) with other probes deployed for shorter timescales with regard to temporal variability (data not shown), indicating that these measurements were representative of conditions across the catchment.

2.4. Data Analysis

2.4.1. Data Validation and Calculation of Nutrient Loads

Unless otherwise specified, all data analysis was conducted using the statistical software R version 3.1.1 [*R Core Team*, 2016]. Servicing, instrument malfunction, and data communication failure led to periodic data losses causing gaps in the measurement time series. Missing data for short gaps <3 h ($n < 20$) were filled by linear interpolation. Longer gaps were not filled and accounted for 7% of the possible 5924 hourly measurements in the monitoring period. NO_3-N and DOC data were smoothed by a running median filter (window width = 8) using the R package *robfilter* to reduce the influence of noise in the time series. In addition to hourly concentration measurements, load time series for NO_3-N and DOC were calculated as

$$P_L = P_C.Q.3600 \quad (1)$$

where P_L is the load for the parameter of interest (mg/hr), P_C is the concentration of the parameter of interest

Table 1. Descriptive Statistics for Explanatory Hydroclimatological Variables Calculated for Each Storm Event[a]

Category	Explanatory Variable	Description	Max	Min	Mean	SD
Flow	t_{Qmax}*	Time from start of event to maximum discharge (h)	25	3	11	6
	Q_{range}	Discharge range during event (L/s)	100	1	26	24
Precipitation	R_{max}*	Maximum rainfall during event within 15 min period (mm)	10	0	3	2
	R_{dur}*	Rainfall duration during event (h)	103	25	50	21
	$Rain_{int}$	Rainfall intensity during event (mm/h)	0.65	0.00	0.24	0.16
	$Rain_{tot}$	Total rainfall during event (mm)	35	0	12	9
Antecedent conditions	$Rain_1$*	Total rainfall in the 1 day prior to event (mm)	9	0	2	2
	$Rain_7$*	Total rainfall in the 7 days prior to event (mm)	65	0	21	17
	$Rain_{14}$	Total rainfall in the 14 days prior to event (mm)	84	1	35	19
	T_{mean14}*	Mean air temperature in the 14 days prior to event (°C)	17	2	12	5
	$Soil_{max7}$*	Maximum soil moisture in the 7 days prior to event (m^3/m^3)	0.48	0.28	0.42	0.06
	GW_{max14}	Maximum groundwater level in the 7 days prior to event (cm)	783	676	729	32
	Δ_{t-1}*	Interval between current event and previous event (h)	499	28	114	117
	Q_{maxt-1}*	Magnitude of previous event (L/s)	117	3	33	27
	DOY*	Day of year	320	87	198	67

[a]Variables marked with an asterisk denote those taken forward for modeling.

(mg/L), and Q is stream discharge at the time of sampling (L/s). Note that for a pure dilution effect of discharge on concentration, the relative changes in P_c and Q compensate to keep P_L constant.

2.4.2. Storm Event Delineation

Storm events were delineated following a rule-based system using the R package *hydromad*. First, the base flow component of the hydrograph was separated using a three pass recursive digital filter with a constant of 0.96 [*Nathan and McMahon*, 1990]. Subsequently, storm events were defined as periods when total stream discharge exceeded base flow by 20% for more than 24 h. No minimum time period between events was stipulated. Only events that had NO_3-N and DOC measurements available for >90% of the duration of the event were considered for analysis. Following the automated selection process, storm event data were examined individually and a small number of outliers were excluded manually based on local site knowledge (e.g., crop irrigation immediately adjacent to the stream resulted in short-term hydropeaking during a dry weather window).

2.4.3. Hydroclimatological Drivers of NO_3-N and DOC Export During Storm Events

Variability in NO_3-N and DOC dynamics between storm events was characterized by calculating the following response variables for each event: maximum event concentration (C_{max}), percent increase and decrease in concentration since the start of the event (P_{inc} and P_{dec}, respectively), and the total load during the event (L_{tot}).

To understand the hydroclimatological processes that drive nutrient dynamics during storm events, specific hydroclimatological variable properties of individual storm events were analyzed (Table 1) with the hypothesis (H_2) that they would provide explanation and predictive capacity for nutrient availability and transport in the catchment. For example, temperature and soil moisture have been previously found to influence the release of nitrogen from organic sources [*Agehara and Warncke*, 2005], while the volume of rainfall before and during an event may be important for creating hydrological connections between catchment nutrient source zones and the stream network. Hydroclimatological variables were examined using a principal component analysis (PCA) with all data standardized and centered prior to analysis using the *ade*4 R package.

To identify the key drivers of nutrient dynamics, we used multiple linear regression and an information-theoretic model selection approach after *Johnson and Omland* [2004]. All data were initially screened for collinearity, and variables with correlation coefficients >0.7 or variance inflation factors >3 were removed from the analysis [*Zuur et al.*, 2010]. Ten predictor variables (R_{max}, R_{dur}, t_{Qmax},$Rain_1$, $Rain_7$, T_{mean14}, $Soil_{max7}$, Δ_{t-1}, Q_{maxt-1}, and day of year (DOY); see Table 1) were then taken forward to fit global models, using ordinary least squares regression, for the five response variables (C_{max}, P_{inc}, P_{dec}, L_{tot}, and hysteresis index—see below) of both NO_3-N and DOC. Predictor variables were transformed where necessary and standardized to improve the interpretability of regression coefficients, i.e., effect sizes [*Schielzeth*, 2010], and the robustness of the statistics. We then fitted all possible subset models of the global model and ranked them using AIC values

(Akaike information criterion). If there was no clear best model (Akaike weight of top model <0.9), model averaging was conducted on all less complex models within AIC <2 of the top model [*Lange et al*., 2014] with regression coefficients calculated as weighted averages [*Burnham and Anderson*, 2003].

2.4.4. Interstorm Variability in NO_3-N and DOC Source Zone Contributions

Analysis of hysteretic behavior between solutes and discharge can provide insights into the sources and transport mechanisms of nutrients within a river catchment [*Bowes et al*., 2005; *Chen et al*., 2012; *Outram et al*., 2014; *Lloyd et al*., 2016b] To better understand the processes controlling nutrient-specific export patterns observed at the catchment outlet (see hypothesis 3), NO_3-N and DOC were characterized as hysteresis indices (HI) for each storm event using methods developed by *Lloyd et al*. [2016a]. The HI for each storm quantifies the "fatness" and direction of the hysteresis loop, whereby clockwise hysteresis behavior is represented by positive HI values and anti clockwise behavior by negative values. Unlike previous methodologies, the HI is calculated for storm data which are first normalized by flow and chemical concentration to enable valid comparisons between storm events with varying concentrations and flow rates. The index is then calculated at multiple points throughout the storm using:

$$HI_{Qi} = C_{RL\_Qi} - C_{FL\_Qi} \quad (2)$$

where HI_{Qi} is the index at percentile i of discharge (Q), C_{RL_Qi} is the chemical value on the rising limb at percentile i of Q, and C_{FL_Qi} is the chemical value at the equivalent point in discharge on the falling limb. The percentiles of discharge (Q_i) are defined by

$$Q_i = k(Q_{max}.Q_{min}) + Q_{min} \quad (3)$$

where Q_{max} is the peak discharge, Q_{min} is the discharge at the start of the event, and k is the point along the loop where the calculation is being made; in this case the index was calculated at every 5% of discharge. Finally, the overall HI was calculated using the mean of the 19 values obtained across the storm loop. HI metrics were regressed against PCA factor scores and NO_3-N and DOC response variables to explore further how changes in hysteresis patterns were linked to hydroclimatological drivers and nutrient dynamics.

3. Results

3.1. Seasonal- and Event-Based Variability in Streamflow, NO_3-N and DOC

The mean stream discharge during the monitoring period was 12.7 L/s. Stream base flow declined gradually from March to August and then rose slightly from mid-August onward (Figure 2a). A total of 568 mm precipitation was recorded. The mean daily precipitation was 3.9 mm and showed no evidence of seasonal variability. Total runoff was 508 mm over the study period with a runoff coefficient of 0.82 (a flow duration curve is presented in Figure S2). Streamflow generally responded rapidly to precipitation inputs; discharge typically increased by >100%, and in some cases up to 400%, within a few h of each rain event, and then returned to base flow conditions over the following 2–3 days. A large increase in discharge occurred over a period of approximately 6 h at the end of the monitoring period following sustained rainfall. Continued monitoring of discharge into December showed that flow conditions returned to base flow after approximately 1 week (data not shown). Air temperature and groundwater level both exhibited strong seasonal patterns and were not influenced to a large extent by short-term storm events. In contrast, soil moisture conditions were highly responsive to precipitation inputs (Figure 2b). In situ measurements of NO_3-N and DOC displayed linear relationships with laboratory measurements (NO_3-N R^2 = 0.97; DOC R^2 = 0.79; Figures S3 and Table S1 in the supporting information). While error associated with the DOC relationship (root-mean-square error (RMSE) = 0.77 mg/L) was greater when compared to NO_3-N (RMSE = 0.37 mg/L), bias was lower (percent bias; 0% versus 3.2%). Mean stream NO_3-N and DOC concentrations were 6.01 mg/L and 12.98 mg/L, respectively, for the entire monitoring period. No long-term trends were observed in NO_3-N concentrations (Figure 2c), but DOC concentrations rose throughout the beginning of the study period, peaked in late August, and then declined through autumn (Figure 2d). DOC exhibited diurnal fluctuations during base flow conditions with peak concentrations in early morning and the lowest concentrations in late afternoon, but this pattern was less evident during storm events (Figure 3). In contrast, diurnal fluctuations in NO_3-N were less apparent.

A total of 36 storm events were identified by the event delineation process, of which 29 were selected for detailed analysis (Figures 2 and S4), covering a range of different hydroclimatological conditions throughout the study period (Table 1). The mean time between events was slightly less than 5 days. Selected storm

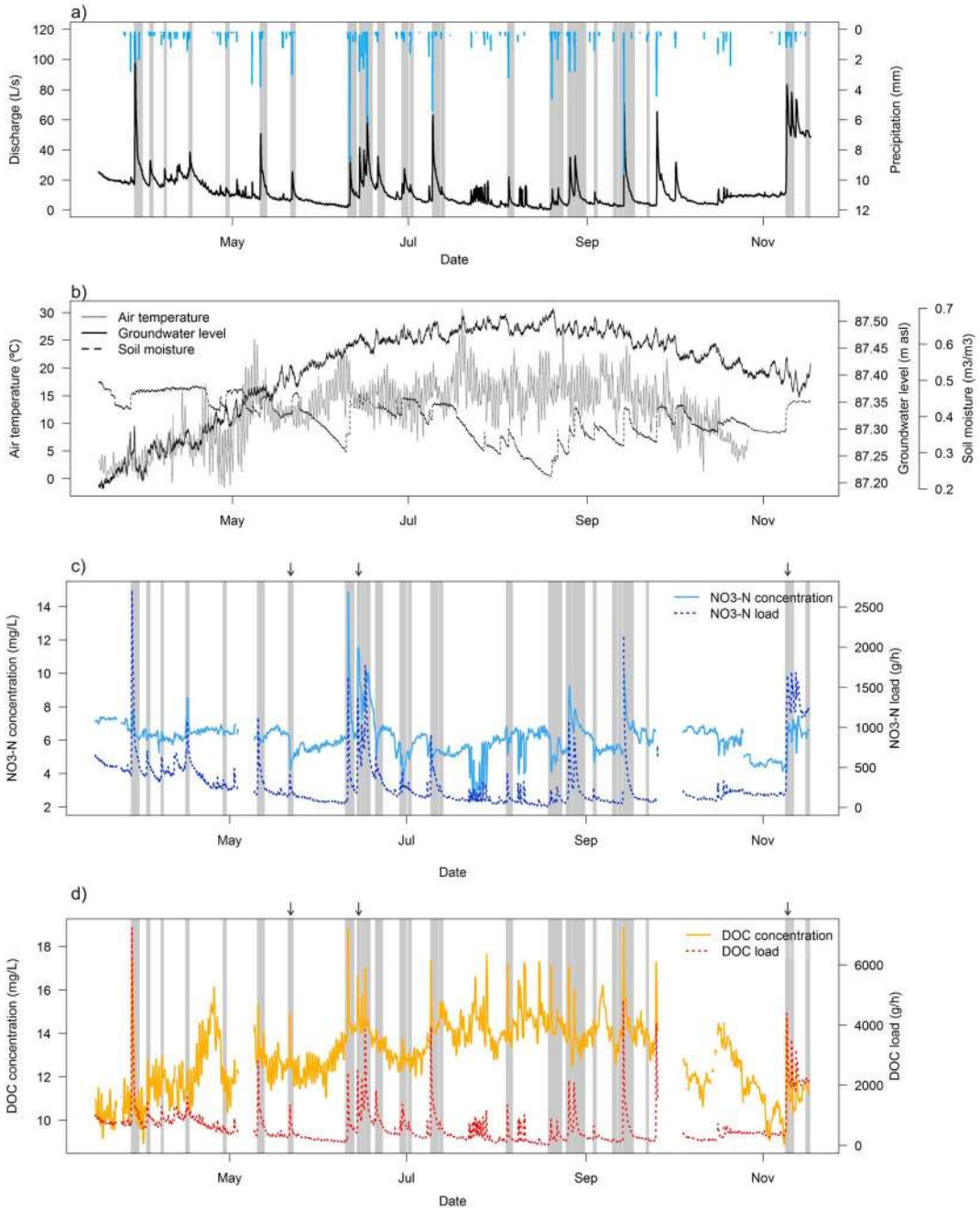

Figure 2. Time series of (a) stream discharge and precipitation, (b) air temperature, groundwater level and soil moisture, (c) NO_3-N concentration and load, and (d) DOC concentration and load. The grey bars denote individual storm events. The arrows above Figures 2c and 2d indicate selected events shown in detail in Figure S5.

events represented 31% of the 248 day monitoring period and accounted for 42% of total NO_3-N and 43% of total DOC exported from the stream catchment during that time. Note, however, that the total number of storms throughout the monitoring period was higher than the 29 selected here for detailed analysis. NO_3-N and DOC concentrations varied between storm events and exhibited both increases and decreases in concentration in response to increased stream discharge (Table 2 and Figure S5). NO_3-N concentrations exhibited an overall increase for 12 of the 29 storm events, while DOC concentrations exhibited an overall increase for 23 events. Mean nutrient concentrations were higher during events than at base flow throughout the monitoring period (Figure 3), albeit with considerable variability around the mean and with limited observations for storms in autumn relative to other seasons. NO_3-N concentrations varied

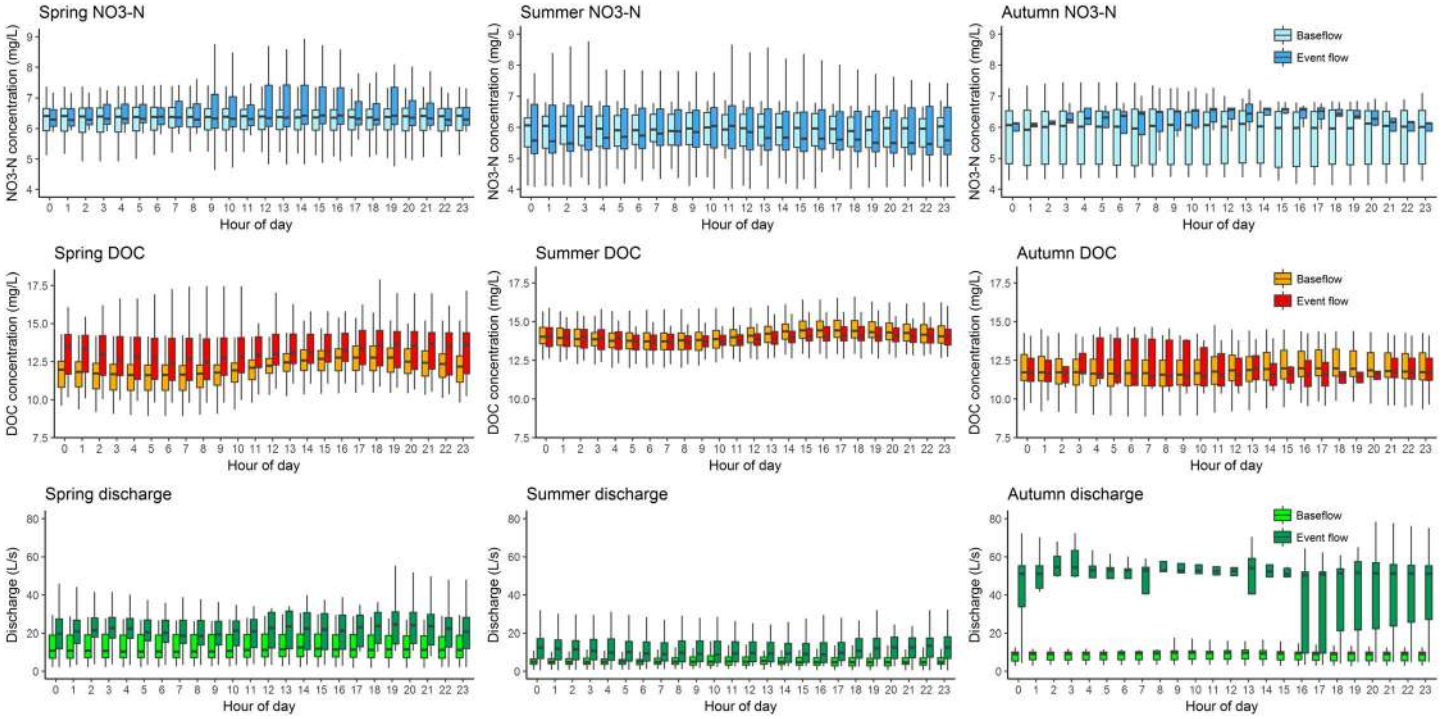

Figure 3. Diel variability in NO_3-N and DOC concentrations and discharge (Q) throughout the monitoring period under base flow and event flow conditions. Seasonal changes are shown by columns for spring (day of year; DOY 75–172; n = 11), summer (DOY 172–265; n = 14), and autumn (DOY 265–322; n = 4).

more intensively between events than DOC: in particular, the mean decrease in NO_3-N concentration throughout all the storm events was 16.2%, compared with 3.2% for DOC (Table 2). In contrast to concentration dynamics, nutrient loads mirrored trends in stream discharge, with both NO_3-N and DOC loads increasing with stream discharge.

PCA analysis of hydroclimatological variables for each storm event produced four components with eigenvalues >1. The first component explained 34% of the variance (Figure 4), with positive loadings for soil moisture and antecedent rainfall and negative loadings for event rainfall duration and time to peak discharge. The second component explained 19% of the variance with positive loadings for total rainfall and discharge range and negative loadings for air temperature and groundwater level. In total, the four components explained 77% of the variance in the data set. Summer storm events generally had negative scores for both axes 1 and 2, while no clear patterns were found for spring and autumn events (Figure 4).

3.2. Hydroclimatological Controls on NO_3-N and DOC Stream Fluxes

NO_3-N and DOC export dynamics were significantly predicted by hydroclimatological variables (Table 3). DOC load was strongly associated with rainfall duration and mean air temperature (effect sizes: 0.57 and −0.53) and moderately associated with soil moisture content (0.37). NO_3-N load was strongly associated with mean air temperature (−0.69) and moderately associated with rain duration and 7 day antecedence (0.44, 0.37). For both DOC and NO_3-N, maximum concentrations were strongly associated with maximum rainfall intensity; however, 7 day antecedence and time since last event were also found to be important for explaining observed NO_3-N dynamics. Concentration increases were associated with maximum rainfall intensity for both nutrients. However, DOC was also influenced by air temperature and rainfall duration, while NO_3-N was influenced by time since last event.

3.3. Variability in NO_3-N and DOC Source Zones Under Different Hydroclimatological Conditions

Clockwise and anticlockwise hysteresis patterns were observed in NO_3-N and DOC concentrations during storm events (Table 2). Examples are presented in Figure 5. Overall, the HI value for NO_3-N exhibited more negative (i.e., anticlockwise) behavior (range −0.8 to 0.69) than the HI for DOC (range −0.66 to 0.94) and

Table 2. Summary of Variability in NO_3-N and DOC Response Variables Observed During Storm Events

	Event Response Variable	Mean	SD	Maximum	Minimum	Range
NO_3-N	Maximum concentration (mg/L)	7.4	2.1	14.9	5.4	9.5
	Increase (%)	12.6	17.5	59.1	0.0	59.1
	Decrease (%)	−16.2	19.1	0.0	−72.9	72.9
	Total load (kg)	22.8	17.8	72.7	1.9	70.8
	Hysteresis index	−0.06	0.49	0.69	−0.80	1.49
DOC	Maximum concentration (mg/L)	15.1	2.0	18.9	11.8	7.1
	Increase (%)	13.9	10.2	40.1	0.0	40.1
	Decrease (%)	−3.2	3.6	0.0	−12.0	12.0
	Total load (kg)	46.6	34.5	143.0	4.7	138.3
	Hysteresis index	0.02	0.32	0.94	−0.66	1.60

was lower on an event-specific basis (mean difference 0.1). The HI for NO_3-N was significantly negatively correlated with PC2 ($r = -0.33$, $p < 0.05$) and PC4 ($r = -0.48$, $p < 0.01$) of the PCA analysis of hydroclimatological variables (as described above and in Figure 4). In contrast, the HI for DOC was not significantly correlated with any PC (Figure 6). No significant correlation was found between the HI for NO_3-N and the HI for DOC ($r = 0.06$, $p > 0.05$). Regression analysis revealed that rainfall antecedence was the strongest control on the HI index for DOC (i.e., greater 7 day rainfall led to increased clockwise hysteresis), although this relationship was still relatively weak when compared to controls on NO_3-N. For NO_3-N mean air temperature and soil water were moderately associated with an increase in clockwise hysteresis, while maximum rainfall and 7 day antecedence were weakly associated with anticlockwise behavior.

4. Discussion

In this study we used high-frequency in situ monitoring to characterize complex nutrient dynamics and unravel connections between hydroclimatological variability and river nutrient export under stormflow conditions. Our results provide new insights into how storm events affect catchment hydrological connectivity and lead to the short-term activation of nutrient-specific source areas that would not otherwise contribute to catchment nutrient fluxes under base flow conditions.

4.1. Temporal Dynamics of Streamflow, NO_3-N, and DOC

We observed temporal variability in streamflow, NO_3-N, and DOC dynamics across a range of temporal scales (i.e., seasonal, diurnal, and event). At the seasonal scale, streamflow decreased through summer in response to relatively warm, yet not unusually dry, conditions with high evapotranspiration potential, and then

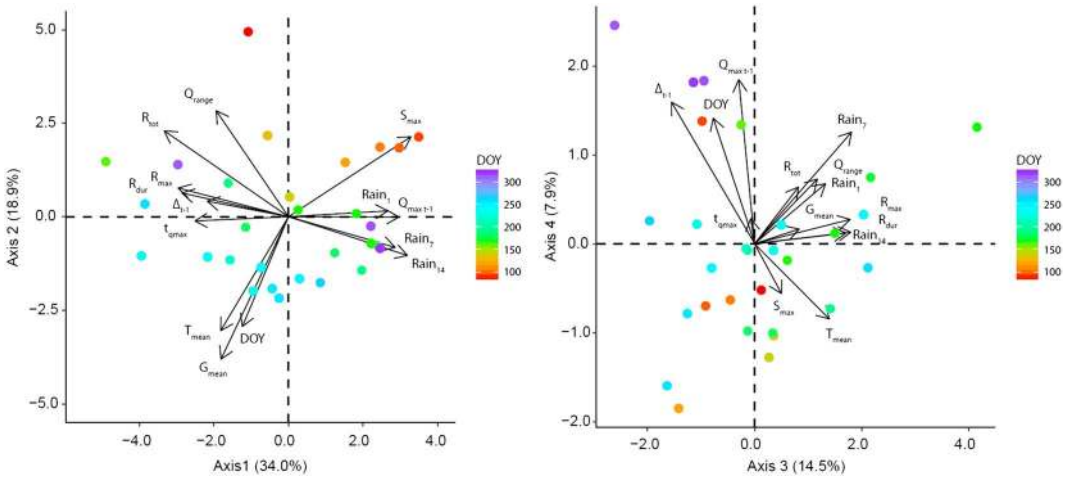

Figure 4. PCA of explanatory hydroclimatological variables for each storm event. Events are colored by day of year (DOY), and loadings of each variable are represented as arrows (magnitude of loading is proportional to arrow length). See Table 1 for full names of explanatory variables.

Table 3. Regression Model Effect Sizes of Hydroclimatological Explanatory Variables on NO_3-N and DOC Response Variables

		Predictor Variables										
	Response Variables	R_{max}	R_{dur}	t_{Qmax}	$Rain_1$	$Rain_7$	T_{mean14}	$Soil_{max7}$	Δ_{t-1}	$Q_{max\ t-1}$	DOY	R^2
DOC	Maximum concentration (mg/L)[a]	0.71										0.58***
	Increase (%)[a]	0.41	0.38				−0.45					0.21*
	Decrease (%)[a]											NS
	Total load (kg)[a]	0.24	0.57				−0.53	0.37			0.27	0.72**
	Hysteresis index[a]				−0.56	0.52						0.21*
NO_3-N	Maximum concentration (mg/L)	0.66				0.41			0.37			0.61***
	Increase (%)	0.47							0.34			0.39*
	Decrease (%)[a]			0.48				0.22				0.31*
	Total load (kg)	0.28	0.44			0.37	−0.69					0.68**
	Hysteresis index	−0.23				−0.26	0.33	0.25				0.51**

[a]Model averaging used for cases when no clear best model was apparent.
*Significance level at $p < 0.05$.
**Significance level at $p < 0.01$.
***Significance level at $p < 0.01$.

increased in autumn. NO_3-N concentrations showed no clear seasonal trend throughout the monitoring period, while for DOC the highest seasonal base flow concentrations (~14 mg/L) were observed in late summer and may have been driven by seasonal inputs of DOM leached from leaf litter in forested areas of the catchment or by release of DOC fixed by instream microbial communities [*Jaffé et al*., 2008]. Such DOC concentrations are akin to those reported for a similar sized agricultural catchment in northern France [*Morel et al*., 2009] but relatively high when compared to values reported from many mixed-use catchments in both Europe and North America [*Raymond and Oh*, 2007; *Monteith et al*., 2007]. Base flow NO_3-N concentrations of around 6.5 mg/L were similar to those reported previously for agricultural catchments [*Lloyd et al*., 2016b; *Thomas et al*., 2016] and were likely driven by current fertilizer application and legacy fertilizer

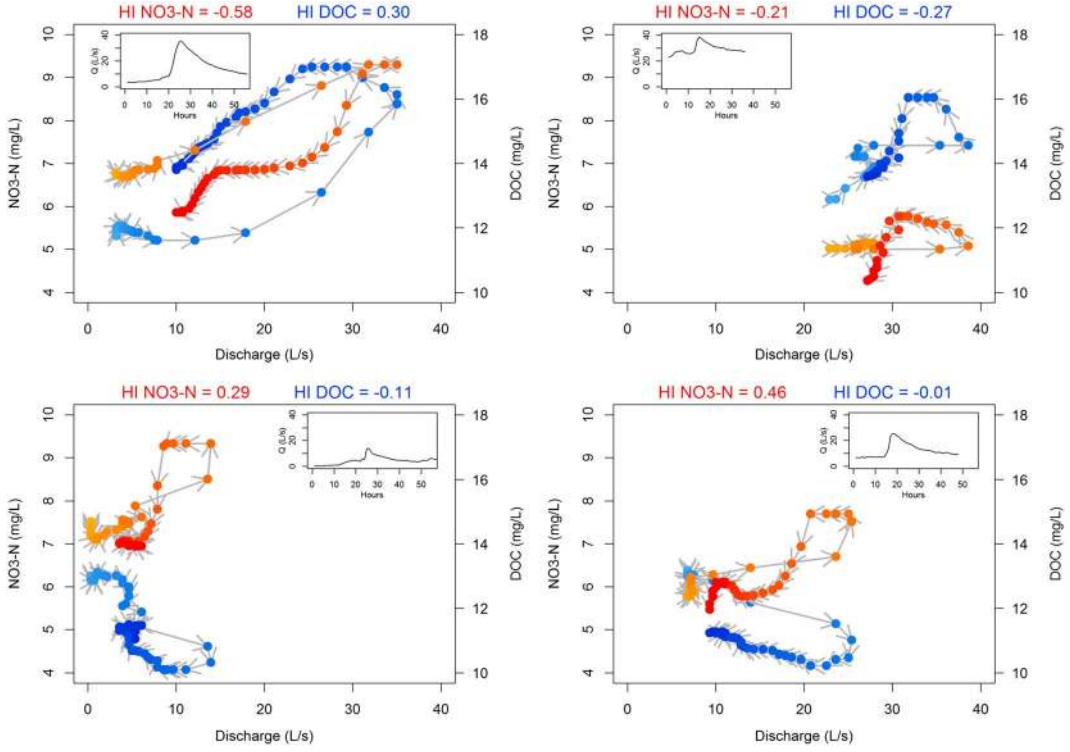

Figure 5. Examples of clockwise (positive HI) and anticlockwise (negative HI) hysteresis patterns observed in NO_3-N and DOC concentrations during selected storm events. The inset panels show the hydrograph for each event. Temporal changes during each event are represented by arrows and color shading (light to dark).

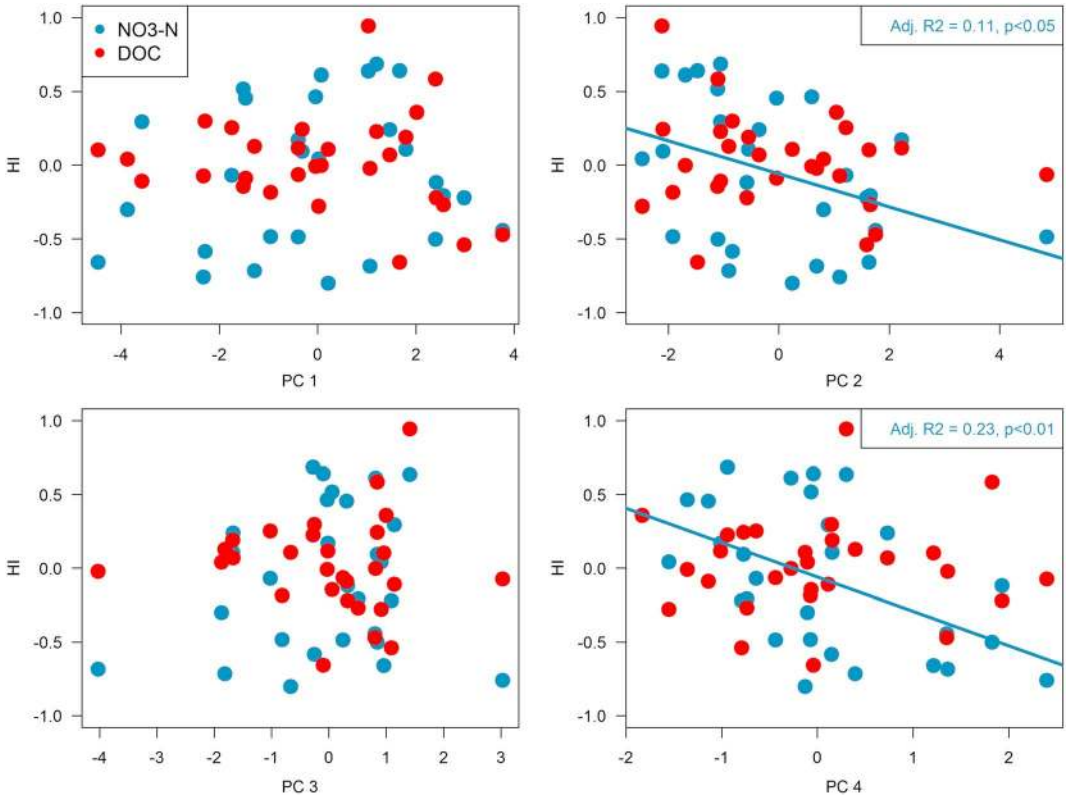

Figure 6. Scatterplots of NO_3-N and DOC hysteresis index (HI) values against principal component scores from PCA of explanatory hydroclimatological variables (see Figure 4).

pollution in arable fields in the upper areas of the catchment, as observed in other parts of the world [*Basu et al*., 2010; *Tesoriero et al*., 2013].

At diurnal scales, streamflow exhibited minor fluctuations during base flow conditions, most likely driven by contrasts in evapotranspiration demand between day and night but also potentially due to temperature-driven changes in water viscosity and associated changes in bed sediment hydraulic conductivity [*Schwab et al*., 2016; *Constantz et al*., 1994]. Observed daily cycles in NO_3-N and DOC concentrations during base flow-dominated periods are likely to reflect a combination of minor dilution effects (in relation to diurnal changes in streamflow) and in-stream assimilatory uptake by microbial communities, which *Rode et al*. [2016a] showed can be high in agricultural catchments compared to those dominated by other land uses. In contrast, photochemical degradation of DOC [e.g., *Spencer et al*., 2007; *Lu et al*., 2013] is unlikely to have had a substantial impact on diel DOC dynamics because the stream channel was incised and shaded by riparian vegetation for much of its length.

Compared to diurnal patterns, storm events induced considerably greater variability in streamflow dynamics and NO_3-N and DOC concentrations, with no evidence for chemostatic behavior during any events [*Moatar et al*., 2017]. The rapid response of streamflow to precipitation inputs can be attributed in part to the numerous ditches and tile drains in the upper catchment. These landscape features have the capacity to export significant quantities of water, and with that nutrients, from agricultural catchments over relatively short time periods [*Li et al*., 2010; *De Schepper et al*., 2015], particularly from areas dominated by clay soils, resulting in flashy hydrological regimes that transfer solutes quickly to fluvial networks [*Bowes et al*., 2005; *Cassidy and Jordan*, 2011]. Responses of NO_3-N and DOC concentration dynamics varied between nutrients and between storm events (as discussed in more detail below). NO_3-N concentrations were typically diluted on the rising limbs of storm hydrographs, most likely due to the rapid delivery of relatively low-concentration water transferred to the stream channel from near-surface soil flow paths in the early stages of each event [*Outram et al*., 2014; *Dupas et al*., 2016], whereas patterns in DOC concentrations generally exhibited flushing behavior through storm events. In contrast to the relatively high variability between NO_3-N and DOC

concentrations, stream solute loads were tightly coupled to discharge for both parameters. This is because the relative change in streamflow during storm events (i.e., orders of magnitude) was substantially higher than the associated change in solute concentration (i.e., multiples), meaning that increases in discharge outweighed dilution effects on concentration (see equation (1)). Therefore, storm events represented important components of the annual hydrograph for mobilization and export of NO_3-N and DOC from the catchment; thus, supporting our first hypothesis that storm events would contribute disproportionately to nutrient export relative to their duration [*Basu et al*., 2010; *Raymond et al*., 2012; *Mellander et al*., 2012]. The insights provided by these high-resolution data sets underscore the value of automated in situ sensors to capture both interevent and intraevent variabilities in storm event dynamics relative to conventional sampling methods using manual grab samples or autosamplers of limited capacity [*Blaen et al*., 2016; *Bowes et al*., 2009].

4.2. Hydroclimatic Drivers of Nutrient Export During Storm Events

In this study, stream nutrient dynamics could be accurately predicted from a relatively small number of variables characterizing the hydroclimatic variability of storm events, incorporating both present and antecedent hydroclimatic conditions, thereby supporting our second hypothesis that hydroclimatological variables would be important predictors of variability in nutrient export. Mean daily precipitation totals were very similar to values reported by *Leeuw et al*. [2015] for precipitation observations across England and Wales, suggesting that our studied storm events are broadly representative of those that occur at a national scale. Precipitation intensity during storm events was particularly important for predicting maximum concentrations and relative increases in concentrations for both NO_3-N and DOC. This is likely due to rapid runoff through the near-surface soil horizon during events of high precipitation intensity, thus mobilizing and routing the product of recently decomposed and nitrified organic matter to the river channel [*Bernal et al*., 2002]. Previous studies have found evidence of nutrient source exhaustion following consecutive storm events [e.g., *Outram et al*., 2016]. We found no evidence of this for DOC; however, the time interval between two events was an additional control on NO_3-N concentrations, with higher maximum and relative increases positively associated with longer time intervals. This suggests that pore water with high concentrations of NO_3-N is flushed from the soil during storm events and that extended dry periods between events are required for mineralization and nitrification of organic N to occur [*Inamdar and Mitchell*, 2006; *Darwiche-Criado et al*., 2015]. Moreover, close linkages between variability in nutrient loads and bulk stream discharge during storm events indicate that aquatic export of both NO_3-N and DOC is primarily transport-limited in this historically agricultural catchment. For NO_3-N, this is most likely to be attributable to the ready surplus of nitrogen derived from current and previous fertilizer use in the upper catchment, which may remain not only in soil horizons but also in groundwater aquifers that are connected hydrologically to the stream [*Krause et al*., 2009]. Transport limitations on NO_3-N export from anthropogenically modified catchments, particularly those impacted by crop management and fertilizer application, have been identified by previous studies [e.g., *Carey et al*., 2014]. Moreover, *Basu et al*. [2010] suggest that such patterns in nutrient export are likely to continue into the future until accumulated legacy stores are depleted. Similarly, DOC export has also been linked to climatic drivers at annual timescales. For example, *Raymond and Saiers* [2010] showed an increase in DOC flux with discharge following a power relationship in forested watersheds in the U.S. However, in contrast, we found a negative relationship between air temperature and DOC load. This may be due to differences in the timing of tree senescence between North America and Europe (i.e., the longer time taken for leaf fall in Europe results in peak DOC leaching later in the season) or alternatively may be caused by larger storm events occurring in spring and autumn months when air temperatures are generally lower at the study site.

4.3. Identification of Nutrient Source Zone Activation Under Contrasting Storm Events

Substantial variation in hysteretic behavior was observed in concentration-discharge relationships between storm events for both NO_3-N and DOC. This variability was quantified through the application of the HI, which enables robust comparison of data between storm events of different magnitudes [*Lloyd et al*., 2016a]. Our modeling results suggested that observed hysteresis patterns were driven by a combination of the hydroclimatological conditions of each particular storm event, coupled with the antecedent hydroclimatological conditions in the period leading up to that event [*Darwiche-Criado et al*., 2015]. For NO_3-N, increased anticlockwise hysteresis patterns were associated with hydroclimatological drivers such as higher rainfall intensity during the event and also with high rainfall and lower air temperature and soil moisture in the preceding

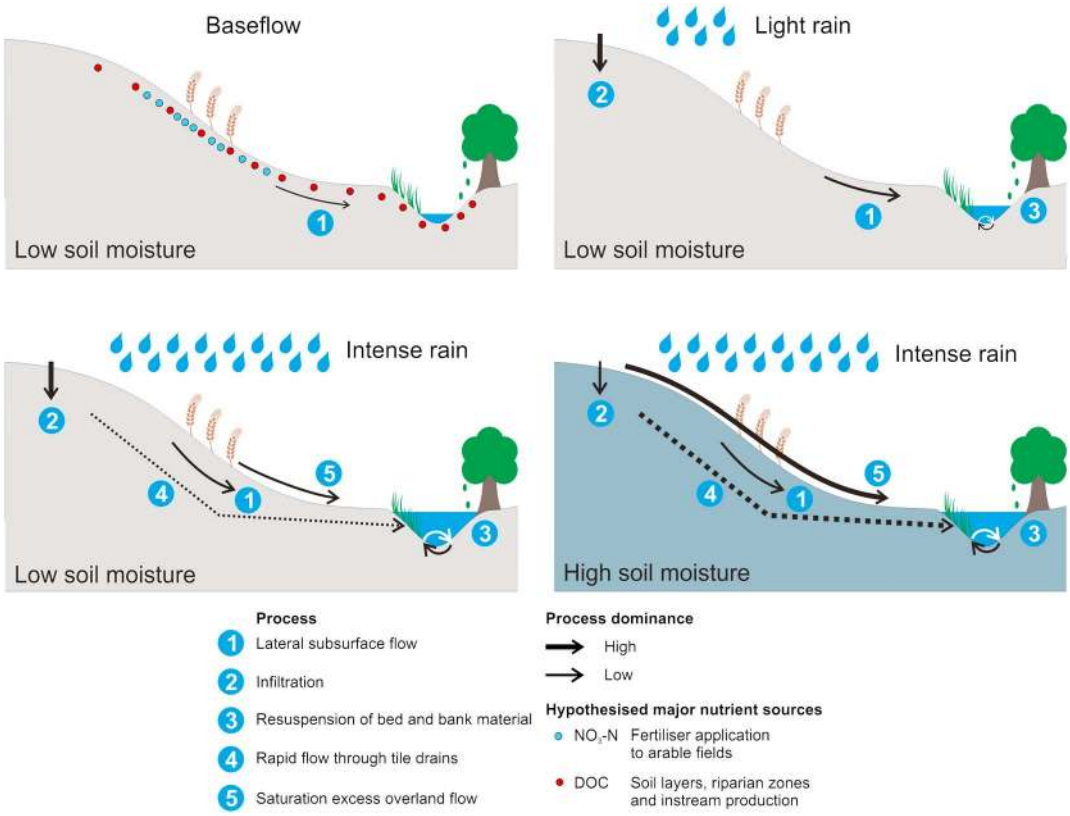

Figure 7. Conceptual model highlighting the spatial distribution of NO_3-N and DOC across the catchment and key processes that control stream nutrient export under different hydroclimatological conditions.

week. For DOC, model results were less significant, but interevent variation in DOC hysteresis behavior appeared to be driven largely by antecedent rainfall rather than by the hydroclimatological conditions experienced throughout each event. However, given the moderate errors associated with the relationship between in situ and paired laboratory measurements of DOC, we suggest that further work is needed to explore carbon export from agricultural catchments. It is likely that different DOM pools of varying quality and composition contribute to the DOC flux causing time-variable relationships between absorbance and DOC quantity. Hence, coupled in situ monitoring of humic- and protein-like fluorescence could improve understanding of DOC behavior under stormflow conditions [*Khamis et al.*, 2017].

Given that neither NO_3-N nor DOC dynamics appeared to be supply-limited in this catchment, as inferred from the tight coupling between streamflow and nutrient loads, it may be assumed that interstorm variability in hysteresis behavior indicates predominantly changes in the activation of different nutrient source zones within the catchment [*Chen et al.*, 2012]. The lack of relationship between the HI for NO_3-N and the HI for DOC reflects differences in the timing of nutrient delivery measured at the catchment outflow, thereby providing strong support for our third hypothesis that nutrient export dynamics would vary between NO_3-N and DOC. This may be associated with both differences in the spatial distribution of nutrient source zones within the catchment and also differences in nutrient-specific transport mechanisms through surface and subsurface flow pathways as summarized in Figure 7.

The most obvious sources of NO_3-N are the current and former arable farmland areas (but also potentially also contaminated groundwater aquifers) in the upper catchment [*Rozemeijer and Broers*, 2007; *Krause et al.*, 2009; *Raymond et al.*, 2012]. As such, NO_3-N hysteresis patterns are hypothesized to reflect hydroclimatological impacts on catchment flow pathways during storm events, resulting in hydrological connectivity and activation of nutrient source zones to the channel network that would not contribute to aquatic NO_3-N export during base flow [*Bowes et al.*, 2009]. This is supported by the observed link between HI and precipitation intensity and antecedent rainfall: thus, certain NO_3-N sources (e.g., those in the surface or

uppermost soil layers) are mobilized when particularly extreme streamflow conditions coincide with high levels of soil saturation. These conditions result in a greater proportion of precipitation converted to overland runoff or preferential flow through subsurface tile drainage networks [*Rozemeijer and Broers*, 2007; *Darwiche-Criado et al*., 2015; *van der Grift et al*., 2016] with corresponding reductions in the influence of catchment subsurface storage on runoff and NO_3-N export dynamics [*Teuling et al*., 2010]. In contrast, during drier periods, lower soil moisture conditions lead to greater infiltration potential, and thus, water and nutrient transport are dominated by subsurface flow pathways (Figure 7).

In contrast to NO_3-N, interpretation of the physical processes underpinning observed hysteresis behavior in DOC was less clear, possibly caused by a more homogenous spatial distribution of DOC across the catchment (e.g., shallow soils, riparian zones, and instream production) relative to that of NO_3-N (Figure 7). However, the tendency of DOC toward more positive (clockwise) hysteresis is suggestive of source areas that are hydrologically well connected to the stream channel with the potential to deliver DOC rapidly at the start of storm events. The low percent bias in the relationship between in situ and laboratory measurements provides confidence in the direction of individual hysteresis patterns. One potential explanation for this behavior is that leaf litter inputs from forested areas of the stream network, particularly in the lower catchment, are entrained and decomposed by microbial communities in hyporheic streambed sediments and then remobilised under high flow conditions (Figure 7), thereby releasing DOC rapidly into the water column [*Bernal et al*., 2002]. This hypothesis is supported by samples acquired from sediment pore waters at 10–20 cm depth in April 2016, when seasonal leaf litter inputs would be expected to be minimal, which showed mean DOC concentrations (25.4 ± 22.3 mg/L) in the streambed to be more than double those in the water column, in some cases up to five times higher (maximum measured DOC concentration 82.6 mg/L). In contrast, N concentrations in the streambed were considerably lower than in the water column, suggesting that streambed sediments were not a major source of NO_3-N to the water column during storm events.

5. Conclusions and Implications

In the context of growing demands on agricultural production and the challenges posed by climate change [*Garnett et al*., 2013], understanding the hydroclimatological drivers of catchment nutrient dynamics, and in particular exports, is critical to developing accurate predictions of water quality in river ecosystems. Our study contributes to this important field of research by developing new mechanistic process understanding from examining interactions between hydroclimatological drivers, streamflow, and nitrogen, and carbon concentrations at high temporal resolution. The use of high-frequency in situ sensors to capture short-term streamflow and solute concentration dynamics through storm events facilitated insights into the processes controlling highly dynamic catchment exports that would be impossible to achieve using discrete sampling methods [*Rode et al*., 2016b; *Blaen et al*., 2016]. Our modeling results highlighted the importance of key hydroclimatological variables, notably rainfall intensity and antecedent conditions, which drive the mobilization and transport of nitrogen and carbon through stream catchments. Given that precipitation regimes in many parts of the world are expected to shift to higher frequencies, and with more extreme events, in the near future [*Kendon et al*., 2014; *Mann et al*., 2017], this finding is important for developing predictive models to assess the potential implications for catchment water quality parameters. As such, our results suggest that management interventions to improve downstream water quality should focus not only on reducing contemporary catchment nutrient inputs (i.e., fertilizer application) but also on developing measures aimed at mitigating the impact of legacy sources that are activated under certain hydroclimatological conditions until their eventual depletion in future. Furthermore, our analysis of differences in nutrient source zone areas indicates that nutrient-specific mitigation measures are required to target particular landscape areas that contribute disproportionately to aquatic nutrient export. These findings highlight the value of high-resolution temporal nutrient time series provided by in situ sensors, as well as the need for more spatially distributed water quality monitoring across river networks to unpick natural system variability. If combined with additional analyses of water age distributions [e.g., *Morgenstern et al*., 2015], particularly at fine temporal resolutions using field analysers [*von Freyberg et al*., 2017], such work will further our ability to assess the relative importance of different nutrient source zones and flow pathways within catchments. Recent advances in sensing technology, coupled with decreasing costs [*Blaen et al*., 2016], mean that high-frequency nutrient measurements from in situ sensors are likely to play an increasingly important role in developing techniques for the effective management of catchment water resources in future.

Acknowledgments
The authors would like to acknowledge support from the Leverhulme Trust (IN-2013-042: International Hyporheic Zone Network: Where rivers, groundwater, and disciplines meet), the UK Natural Environment Research Council (NERC NE/L003872/1), the University of Birmingham, the Birmingham Institute of Forest Research (BIFoR paper #28), and the JABBS Foundation. We extend our thanks to the Norbury Park Estate for access to their land and to John Braithwaite for providing farming records. We also thank two anonymous reviewers for comments that improved the manuscript. All data supporting our conclusions are available freely at https://figshare.com/s/d32f4c1f8d6cb8fd965c.

References

Agehara, S., and D. Warncke (2005), Soil moisture and temperature effects on nitrogen release from organic nitrogen sources, *Soil Sci. Soc. Am. J.*, *69*, 1844–1855.

Basu, N. B., G. Destouni, J. W. Jawitz, S. E. Thompson, N. V. Loukinova, A. Darracq, S. Zanardo, M. Yaeger, M. Sivapalan, and A. Rinaldo (2010), Nutrient loads exported from managed catchments reveal emergent biogeochemical stationarity, *Geophys. Res. Lett.*, *37*, L23404, doi:10.1029/2010GL045168.

Bennett, E. M., G. D. Peterson, and L. J. Gordon (2009), Understanding relationships among multiple ecosystem services, *Ecol. Lett.*, *12*, 1394–1404.

Bernal, S., A. Butturini, and F. Sabater (2002), Variability of DOC and nitrate responses to storms in a small Mediterranean forested catchment, *Hydrol. Earth Syst. Sci. Discuss.*, *6*, 1031–1041.

Bieroza, M., A. Heathwaite, N. Mullinger, and P. Keenan (2014), Understanding nutrient biogeochemistry in agricultural catchments: The challenge of appropriate monitoring frequencies, *Environ. Sci. Processes Impacts*, *16*, 1676–1691.

Bishop, K., C. Pettersson, B. Allard, and Y.-H. Lee (1994), Identification of the riparian sources of aquatic dissolved organic carbon, *Environ. Int.*, *20*, 11–19.

Blaen, P., K. Khamis, C. Lloyd, C. Bradley, and S. Krause (2016), Real-time monitoring of nutrients and dissolved organic matter in rivers: Adaptive monitoring strategies, technological challenges and future directions, *Sci. Total Environ.*, *569*, 647–660.

Bowes, M. J., W. A. House, R. A. Hodgkinson, and D. V. Leach (2005), Phosphorus-discharge hysteresis during storm events along a river catchment: The river swale, UK, *Water Res.*, *39*, 751–762.

Bowes, M. J., J. T. Smith, and C. Neal (2009), The value of high-resolution nutrient monitoring: A case study of the River Frome, Dorset, UK, *J. Hydrol.*, *378*, 82–96.

Burnham, K. P., and D. R. Anderson (2003) *Model Selection and Multimodel Inference: A Practical Information-Theoretic Approach*, Springer Science & Business Media, Bertlin.

Burt, T., N. Howden, F. Worrall, and M. Whelan (2010), Long-term monitoring of river water nitrate: How much data do we need?, *J. Environ. Monit.*, *12*, 71–79.

Carey, R. O., W. M. Wollheim, G. K. Mulukutla, and M. M. Mineau (2014), Characterizing storm-event nitrate fluxes in a fifth order suburbanizing watershed using in situ sensors, *Environ. Sci. Technol.*, *48*, 7756–7765.

Carpenter, K., T. Kraus, J. Goldman, J. F. Saracen, B. Downing, and B. Bergamaschi (2013), Sources and characteristics of organic matter in the Clackamas River, Oregon, related to the formation of disinfection by-products in treated drinking water, Water Research Foundation Denver.

Cassidy, R., and P. Jordan (2011), Limitations of instantaneous water quality sampling in surface-water catchments: Comparison with near-continuous phosphorus time-series data, *J. Hydrol.*, *405*, 182–193.

Chen, N., J. Wu, and H. Hong (2012), Effect of storm events on riverine nitrogen dynamics in a subtropical watershed, southeastern China, *Sci. Total Environ.*, *431*, 357–365.

Constantz, J., C. L. Thomas, and G. Zellweger (1994), Influence of diurnal variations in stream temperature on streamflow loss and groundwater recharge, *Water Resour. Res.*, *30*, 3253–3264.

Darwiche-Criado, N., F. A. Comín, R. Sorando, and J. M. Sánchez-Pérez (2015), Seasonal variability of NO_3^- mobilization during flood events in a Mediterranean catchment: The influence of intensive agricultural irrigation, *Agric. Ecosyst. Environ.*, *200*, 208–218.

De Schepper, G., R. Therrien, J. C. Refsgaard, and A. L. Hansen (2015), Simulating coupled surface and subsurface water flow in a tile-drained agricultural catchment, *J. Hydrol.*, *521*, 374–388.

Drewry, J., L. Newham, and B. Croke (2009), Suspended sediment, nitrogen and phosphorus concentrations and exports during storm-events to the Tuross estuary, Australia, *J. Environ. Manage.*, *90*, 879–887.

Dupas, R., S. Jomaa, A. Musolff, D. Borchardt, and M. Rode (2016), Disentangling the influence of hydroclimatic patterns and agricultural management on river nitrate dynamics from sub-hourly to decadal time scales, *Sci. Total Environ.*, *571*, 791–800.

Friberg, N., J. Skriver, S. E. Larsen, M. L. Pedersen, and A. Buffagni (2010), Stream macroinvertebrate occurrence along gradients in organic pollution and eutrophication, *Freshw. Biol.*, *55*, 1405–1419.

Garner, G., A. F. Van Loon, C. Prudhomme, and D. M. Hannah (2015), Hydroclimatology of extreme river flows, *Freshw. Biol.*, *60*, 2461–2476.

Garnett, T., M. Appleby, A. Balmford, I. Bateman, T. Benton, P. Bloomer, B. Burlingame, M. Dawkins, L. Dolan, and D. Fraser (2013), Sustainable intensification in agriculture: Premises and policies, *Science*, *341*, 33–34.

Grabs, T., K. Bishop, H. Laudon, S. W. Lyon, and J. Seibert (2012), Riparian zone hydrology and soil water total organic carbon (TOC): Implications for spatial variability and upscaling of lateral riparian TOC exports, *Biogeosciences*, *9*, 3901–3916.

Gruber, N., and J. N. Galloway (2008), An Earth -system perspective of the global nitrogen cycle, *Nature*, *451*, 293–296.

Halliday, S. J., R. A. Skeffington, A. J. Wade, M. J. Bowes, E. Gozzard, J. R. Newman, M. Loewenthal, E. J. Palmer-Felgate, and H. P. Jarvie (2015), High-frequency water quality monitoring in an urban catchment: Hydrochemical dynamics, primary production and implications for the Water Framework Directive, *Hydrol. Process.*, *29*, 3388–3407.

Huang, W., and R. F. Chen (2009), Sources and transformations of chromophoric dissolved organic matter in the Neponset River Watershed, *J. Geophys. Res.*, *114*, G00F05, doi:10.1029/2009JG000976.

Hudson, R., and J. Fraser (2005), The mass balance (or dry injection) method, *Streamline Watershed Manage. Bull.*, *9*, 6–12.

Inamdar, S. P., and M. J. Mitchell (2006), Hydrologic and topographic controls on storm-event exports of dissolved organic carbon (DOC) and nitrate across catchment scales, *Water Resour. Res.*, *42*, W03421, doi:10.1029/2005WR004212.

Jaffé, R., D. Mcknight, N. Maie, R. Cory, W. Mcdowell, and J. Campbell (2008), Spatial and temporal variations in DOM composition in ecosystems: The importance of long-term monitoring of optical properties, *J. Geophys. Res.*, *113*, G04032, doi:10.1029/2008JG000683.

Johnson, J. B., and K. S. Omland (2004), Model selection in ecology and evolution, *Trends Ecol. Evol.*, *19*, 101–108.

Kendon, E. J., N. M. Roberts, H. J. Fowler, M. J. Roberts, S. C. Chan, and C. A. Senior (2014), Heavier summer downpours with climate change revealed by weather forecast resolution model, *Nat. Clim. Change*, *4*, 570–576.

Khamis, K., C. Bradley, R. Stevens, and D. M. Hannah (2017), Continuous field estimation of dissolved organic carbon concentration and biochemical oxygen demand using dual-wavelength fluorescence, turbidity and temperature, *Hydrol. Process.*, *31*, 540–555.

Krause, S., L. Heathwaitev, A. Binley, and P. Keenan (2009), Nitrate concentration changes at the groundwater-surface water interface of a small Cumbrian river, *Hydrol. Process.*, *23*, 2195–2211.

Krause, S., J. Lewandowski, C. N. Dahm, and K. Tockner (2015), Frontiers in real-time ecohydrology–a paradigm shift in understanding complex environmental systems, *Ecohydrology*, *8*(4), 529–537.

Lange, K., C. R. Townsend, R. Gabrielsson, P. Chanut, and C. D. Matthaei (2014), Responses of stream fish populations to farming intensity and water abstraction in an agricultural catchment, *Freshw. Biol.*, *59*, 286–299.
Leeuw, J., J. Methven, and M. Blackburn (2015), Variability and trends in England and Wales precipitation, *Int. J. Climatol.*, *36*(8), 2823–2836.
Li, H., M. Sivapalan, F. Tian, and D. Liu (2010), Water and nutrient balances in a large tile-drained agricultural catchment: A distributed modeling study, *Hydrol. Earth Syst. Sci.*, *14*, 2259–2275.
Lloyd, C., J. Freer, P. Johnes, and A. Collins (2016a), Technical note: Testing an improved index for analysing storm discharge–concentration hysteresis, *Hydrol. Earth Syst. Sci.*, *20*, 625–632.
Lloyd, C. E. M., J. E. Freer, P. J. Johnes, and A. L. Collins (2016b), Using hysteresis analysis of high-resolution water quality monitoring data, including uncertainty, to infer controls on nutrient and sediment transfer in catchments, *Sci. Total Environ.*, *543*(Part A), 388–404.
Lu, Y., J. E. Bauer, E. A. Canuel, Y. Yamashita, R. Chambers, and R. Jaffé (2013), Photochemical and microbial alteration of dissolved organic matter in temperate headwater streams associated with different land use, *J. Geophys. Res. Biogeosci.*, *118*, 566–580, doi:10.1002/jgrg.20048.
Mann, M. E., S. Rahmstorf, K. Kornhuber, B. A. Steinman, S. K. Miller, and D. Coumou (2017), Influence of anthropogenic climate change on planetary wave resonance and extreme weather events, *Sci. Rep.*, *7*, doi:10.1038/srep45242.
Mellander, P.-E., A. R. Melland, P. Jordan, D. P. Wall, P. N. Murphy, and G. Shortle (2012), Quantifying nutrient transfer pathways in agricultural catchments using high temporal resolution data, *Environ. Sci. Pol.*, *24*, 44–57.
Millennium Ecosystem Assessment (2005), Ecosystems and human well-being, Washington, D. C.
Moatar, F., B. Abbott, C. Minaudo, F. Curie, and G. Pinay (2017), Elemental properties, hydrology, and biology interact to shape concentration-discharge curves for carbon, nutrients, sediment, and major ions, *Water Resour. Res.*, *53*, 1270–1287, doi:10.1002/2016WR019635.
Monteith, D. T., J. L. Stoddard, C. D. Evans, H. A. De Wit, M. Forsius, T. Høgåsen, A. Wilander, B. L. Skjelkvåle, D. S. Jeffries, and J. Vuorenmaa (2007), Dissolved organic carbon trends resulting from changes in atmospheric deposition chemistry, *Nature*, *450*, 537–540.
Morel, B., P. Durand, A. Jaffrezic, G. Gruau, and J. Molénat (2009), Sources of dissolved organic carbon during stormflow in a headwater agricultural catchment, *Hydrol. Process.*, *23*, 2888–2901.
Morgenstern, U., C. J. Daughney, G. Leonard, D. Gordon, F. M. Donath, and R. Reeves (2015), Using groundwater age and hydrochemistry to understand sources and dynamics of nutrient contamination through the catchment into Lake Rotorua, New Zealand, *Hydrol. Earth Syst. Sci.*, *19*, 803–822.
Nathan, R., and T. Mcmahon (1990), Evaluation of automated techniques for base flow and recession analyses, *Water Resour. Res.*, *26*, 1465–1473.
Norby, R. J., M. G. De Kauwe, T. F. Domingues, R. A. Duursma, D. S. Ellsworth, D. S. Goll, D. M. Lapola, K. A. Luus, A. R. Mackenzie, and B. E. Medlyn (2016), Model–data synthesis for the next generation of forest free-air CO2 enrichment (FACE) experiments, *New Phytol.*, *209*, 17–28.
Outram, F., C. Lloyd, J. Jonczyk, C. M. Benskin, F. Grant, M. Perks, C. Deasy, S. Burke, A. Collins, and J. Freer (2014), High-frequency monitoring of nitrogen and phosphorus response in three rural catchments to the end of the 2011–2012 drought in England, *Hydrol. Earth Syst. Sci.*, *18*, 3429–3448.
Outram, F. N., R. J. Cooper, G. Sünnenberg, K. M. Hiscock, and A. A. Lovett (2016), Antecedent conditions, hydrological connectivity and anthropogenic inputs: Factors affecting nitrate and phosphorus transfers to agricultural headwater streams, *Sci. Total Environ.*, *545*, 184–199.
Pacific, V. J., K. G. Jencso, and B. L. Mcglynn (2010), Variable flushing mechanisms and landscape structure control stream DOC export during snowmelt in a set of nested catchments, *Biogeochemistry*, *99*, 193–211.
Pellerin, B. A., J. F. Saraceno, J. B. Shanley, S. D. Sebestyen, G. R. Aiken, W. M. Wollheim, and B. A. Bergamaschi (2012), Taking the pulse of snowmelt: In situ sensors reveal seasonal, event and diurnal patterns of nitrate and dissolved organic matter variability in an upland forest stream, *Biogeochemistry*, *108*, 183–198.
R Core Team (2016), R: A language and environment for statistical computing, R Foundation for Statistical Computing, Vienna, Austria. 2015. [Available at www.R-project.org.]
Raymond, P. A., and N. H. Oh (2007), An empirical study of climatic controls on riverine C export from three major US watersheds, *Global Biogeochem. Cycles*, *21*, GB2022, doi:10.1029/2006GB002783.
Raymond, P. A., and J. E. Saiers (2010), Event controlled DOC export from forested watersheds, *Biogeochemistry*, *100*, 197–209.
Raymond, P. A., M. B. David, and J. E. Saiers (2012), The impact of fertilization and hydrology on nitrate fluxes from Mississippi watersheds, *Curr. Opin. Environ. Sustain.*, *4*, 212–218.
Ritson, J., N. Graham, M. Templeton, J. Clark, R. Gough, and C. Freeman (2014), The impact of climate change on the treatability of dissolved organic matter (DOM) in upland water supplies: A UK perspective, *Sci. Total Environ.*, *473*, 714–730.
Rode, M., S. Halbedel NéE Angelstein, M. R. Anis, D. Borchardt, and M. Weitere (2016a), Continuous in-stream assimilatory nitrate uptake from high-frequency sensor measurements, *Environ. Sci. Technol.*, *50*, 5685–5694.
Rode, M., A. J. Wade, M. J. Cohen, R. T. Hensley, M. J. Bowes, J. W. Kirchner, G. B. Arhonditsis, P. Jordan, B. Kronvang, and S. J. Halliday (2016b), Sensors in the stream: The high-frequency wave of the present, *Environ. Sci. Technol.*, *50*, 10,297–10,307.
Rozemeijer, J., and H. Broers (2007), The groundwater contribution to surface water contamination in a region with intensive agricultural land use (Noord-Brabant, The Netherlands), *Environ. Pollut.*, *148*, 695–706.
Saraceno, J. F., B. A. Pellerin, B. D. Downing, E. Boss, P. A. Bachand, and B. A. Bergamaschi (2009), High-frequency in situ optical measurements during a storm event: Assessing relationships between dissolved organic matter, sediment concentrations, and hydrologic processes, *J. Geophys. Res. 114*, G00F09, doi:10.1029/2009JG000989.
Schielzeth, H. (2010), Simple means to improve the interpretability of regression coefficients, *Methods Ecol. Evol.*, *1*, 103–113.
Schwab, M., J. Klaus, L. Pfister, and M. Weiler (2016), Diel discharge cycles explained through viscosity fluctuations in riparian inflow, *Water Resour. Res.*, *52*, 8744–8755, doi:10.1002/2016WR018626.
Smith, V. H., and D. W. Schindler (2009), Eutrophication science: Where do we go from here?, *Trends Ecol. Evol.*, *24*, 201–207.
Spencer, R. G., B. A. Pellerin, B. A. Bergamaschi, B. D. Downing, T. E. Kraus, D. R. Smart, R. A. Dahlgren, and P. J. Hernes (2007), Diurnal variability in riverine dissolved organic matter composition determined by in situ optical measurement in the San Joaquin River (California, USA), *Hydrol. Process.*, *21*, 3181–3189.
Tesoriero, A. J., J. H. Duff, D. A. Saad, N. E. Spahr, and D. M. Wolock (2013), Vulnerability of streams to legacy nitrate sources, *Environ. Sci. Technol.*, *47*, 3623–3629.
Teuling, A., I. Lehner, J. Kirchner, and S. Seneviratne (2010), Catchments as simple dynamical systems: Experience from a Swiss prealpine catchment, *Water Resour. Res.*, *46*, W10502, doi:10.1029/2009WR008777.
Thomas, Z., B. W. Abbott, O. Troccaz, J. Baudry, and G. Pinay (2016), Proximate and ultimate controls on carbon and nutrient dynamics of small agricultural catchments, *Biogeosciences*, *13*, 1863–1875.

Van Der Grift, B., H. P. Broers, W. Berendrecht, J. Rozemeijer, L. Osté, and J. Griffioen (2016), High-frequency monitoring reveals nutrient sources and transport processes in an agriculture-dominated lowland water system, *Hydrol. Earth Syst. Sci.*, *20*, 1851–1868.

Von Freyberg, J., B. Studer, and J. W. Kirchner (2017), A lab in the field: High-frequency analysis of water quality and stable isotopes in stream water and precipitation, *Hydrol. Earth Syst. Sci.*, *21*, 1721.

Wade, A. J., E. Palmer-Felgate, S. J. Halliday, R. A. Skeffington, M. Loewenthal, H. Jarvie, M. Bowes, G. Greenway, S. Haswell, and I. Bell (2012), Hydrochemical processes in lowland rivers: Insights from in situ, high-resolution monitoring, *Hydrol. Earth Syst. Sci.*, *16*, 4323–4342.

Wang, G., D. Wang, K. E. Trenberth, A. Erfanian, M. Yu, M. G. Bosilovich, and D. T. Parr (2017), The peak structure and future changes of the relationships between extreme precipitation and temperature, *Nat. Clim. Change*, *7*(4), 268–274.

Ward, M. H., T. M. Dekok, P. Levallois, J. Brender, G. Gulis, B. T. Nolan, and J. Vanderslice (2005), Workgroup report: Drinking-water nitrate and health-recent findings and research needs, *Environ. Health Perspect.*, 1607–1614.

Wilson, H. F., J. E. Saiers, P. A. Raymond, and W. V. Sobczak (2013), Hydrologic drivers and seasonality of dissolved organic carbon concentration, nitrogen content, bioavailability, and export in a forested New England stream, *Ecosystems*, *16*, 604–616.

Zuur, A. F., E. N. Ieno, and C. S. Elphick (2010), A protocol for data exploration to avoid common statistical problems, *Methods Ecol. Evol.*, *1*, 3–14.